JurnalPolimesin
Department of Mechanical Engineering
State Polytechnic of Lhokseumawe
http://e-jurnal.pnl.ac.id/polimesin
e-ISSN : 2549-1999 No. : 5 Month : October
p-ISSN : 1693-5462 Volume : 21 Year : 2023

Article Processing Dates: Received on 2023-07-07, Reviewed on 2023-08-02, Revised on 2023-09-14, Accepted on 2023-10-13 and Available online on 2023-10-29

Mobility, Kinematic, Singularity, And Workspace Analysis Of a Translational Parallel Manipulator With 2(RRPaRR)-PRRR Kinematic Chains

Indra Hasan, Adriyan*, Deru Assadullah Hanif, Daniel Rumahorbo, Bima Amrianto Rahmad Illahiy
Department of Mechanical Engineering, Universitas Muhammadiyah Riau, Pekanbaru, 28292, Indonesia
*Corresponding author: adriyan@umri.ac.id

Abstract

This article presents an asymmetric parallel manipulator with 2(RRPaRR)-PRRR kinematic chains. This manipulator aims to operate as a lower-mobility parallel manipulator with the pure translational motion of its platform. Therefore, a series of analyses are performed to fulfill this intention. First, the mobility analysis is performed by applying the Grübler-Kutzbach equation and the screw theory. Then, the kinematic, singularity, and workspace analysis are applied to analyze this PM. As a result, the application of the screw theory for the configuration of its kinematic chains shows its mobility in a pure translational motion in space. Then, this manipulator has a closed-form solution for its direct kinematic problem expressed in a quadratic equation. By applying singularity and workspace analysis via visualization, the singularity-free workspace along the z-axis of its workspace can be identified. This can later be used as a useful workspace. Overall, the presented manipulator can be applied to a translational parallel manipulator.

Keywords:
Mobility, singularity, workspace, 2(RRPaRR)-PRRR kinematic chains, and translational parallel manipulators.

1 Introduction

Parallel manipulators – PMs in brief – employ closed-loop kinematic chains for the transmission of motions and forces/torques from the actuators to their end effectors. This type of manipulator provides great benefits compared to its peer, the serial manipulators. These benefits are low positioning error, high velocities, high acceleration, high ratio of load to its weight, and high dynamic characteristics [1]. The primary disbenefit is the small size of its workspace and the existence of a singularity within its workspace. To counteract this disbenefit, the optimization techniques can be applied to obtain optimal dimensions as reported by [2]–[4].

In terms of the mobility or Degrees of Freedom (DoF) of the end effectors (or the platforms), the PMs can be distinguished between full mobility and lower-mobility. The full mobility means that the end effector of the PMs can fully undergo three translations (3T) and three rotations (3R) in space. The PMs with this feature allow the manipulation of an object on its end effector in a general spatial motion, for example a novel 3-RRUU 6-DoF PM [5]. Meanwhile, some practical applications only require an object to be manipulated less than six or the general spatial motion. Therefore, these applications will rely on lower-mobility PMs with simpler architecture and controller [6].

The research on the lower-mobility PMs has evolved over the past three decades. It was marked by the invention of the Delta Parallel Manipulator – DPM for short – by Clavel in the early 90's [7]. This manipulator has characteristics such as pure translational motion in space (3T), high speeds, and high accelerations. To date, a great deal of research has been devoted to gaining a better understanding of this manipulator in the areas of kinematics, dynamics, dimensional synthesis [8], [9], motion error [10], [11], and motion reliability [12], to name a few.

In addition, other architectures have been designed to achieve the same mobility as the DPM. The well-known 3-PRRR kinematic chain has been studied for more than twenty years. This type of manipulator is classified as an isotropic PM because its Jacobian matrix is a unit matrix. The most recent studies show the application of this PM for lower-limb rehabilitation [13]. Subsequently, the largest interference-free workspace of this PM for such rehabilitation is investigated by the same authors in [14]. Later, they develop a control strategy for a prototype of this PM [15].

The two pure translational PMs presented previously are symmetric PMs because they have the same kinematic chains on each limb. Their other counterpart is the asymmetric pure translational PM, which has different kinematic chains on each limb. These asymmetric PMs have been less studied compared to their peers. Shen et al. presented a topological design for the asymmetric pure translational PMs with an RPa(3R) 2R+RPa kinematic chain [16]. They had discussed a finding about this manipulator for its decoupled characteristic, which gave a simple derivation for inverse and direct kinematics, and a simple representation for its singular condition. Another asymmetric pure translational PM with PLMEs (parallel linear motion elements) and 2(UPR) kinematic chain was proposed by Yang et al. for a pick-and-place operation with heavy load [17]. This manipulator was designed to have a simpler structure and higher transmission efficiency than the other purely translational PMs.

In short, the literature reviews presented so far show that the symmetric and asymmetric PMs use the same type of actuator for each limb, i.e. all rotary or all linear actuators. In this research, an attempt is made to propose an asymmetric parallel manipulator that uses a combination of RRPaRR and PRRR kinematic chains with different types of actuators on each limb. Then, a study is carried out to investigate this manipulator with such a kinematic chain. The steps are applied. First of all, such a kinematic chain has to be set up and its mobility is analyzed by using the Grübler-Kutzbach (GK) equation and the screw theory. Finally, the analysis of the kinematics, the singularity, and the workspace can be performed to obtain their mathematical relations and the visualization of the workspace.

2 Research Methods

First, this research is carried out by selecting a possible kinematic chain to be applied to the asymmetric parallel manipulator. For this purpose, a 2(RRPaRR)-PRRR kinematic chain is selected and used, as shown in Fig. 1. Here, R, P, and Pa stand for revolute joint, prismatic joint, and parallelogram chain, respectively. In addition, the parallelogram chain consists of four binary links that are perpendicular to each other and connected to four revolute joints. An underscore below the joint letter indicates the actuated or active joint. This manipulator has three limbs, the first two of which have the same kinematic structure, i.e. RRPaRR, while the last limb has a kinematic chain of PRRR.

Next, the mobility of the manipulator can be determined using the information reserved by the kinematic chain. This mobility can be calculated in two ways, i.e.: the Grübler-Kutzbach (GK) equation and the screw theory. The GK equation takes the number of links and joints possessed by the manipulator for the mobility calculation. On the other hand, the screw theory can be applied by

constructing unit motion screws (unit twists) of each joint in the first step. Each twist at the respective joint is formed by its unit direction vector and its position vector concerning point *O* on the *XYZ* of the fixed reference of the frame. Once the twists are formed at each joint, they can be arranged for each limb as well. This arrangement is then referred to as the Limb Twist System (LTS).

Once the LTSs are established, the unit wrench system acting on each limb can be obtained, referred to as a Limb Wrench System (LWS). Each LWS is obtained by applying a reciprocal screw product to each respective LTS. These LWSs are then combined to form the unit wrench acting on the platform. It is here that the Platform Wrench System (PWS) is subsequently formed. Applying the reciprocal screw product to the PWS again results in the unit twist system of the platform and is referred to as the Platform Twist System (PTS). Finally, the manipulator mobility can be inferred in terms of number, direction, and type. Thus, this number correlates to the number of unit twists in the PWS. The direction can be determined whether it is translation along or rotation around the *X*, *Y*, and *Z*-axis.

Once how the platform moves in the space has been determined, it is possible to proceed to the kinematic analysis of the manipulator. This kinematic analysis consists of position analysis (the inverse and direct kinematic problem) and velocity analysis.Both the inverse and direct kinematic problem can be analyzed using vector analysis with reference to the geometry of PM as shown in Fig. 1. It provides a mathematical relation between end-effector space on the platform and actuator space. The inverse kinematic problem can be solved analytically to obtain a closed-form solution of the actuator space for the known end-effector space.

On the contrary, the direct kinematic problem yields a solution for the end-effector space if the actuator space is specified. The direct kinematic solution can be a closed-form solution if one exists, or it can be determined through numerical methods. This research presents both solutions that are closed-form and numerical solutions. The closed-form solution is determined by applying the dyallitic elimination method, while the numerical solution is sought by implementing the interval analysis method. The interval analysis method ensures a bounded solution that envelopes the closed-form solution. It implies that the closed-form solution lies somewhere within this interval solution. The reference in [18]–[20] provides an in-depth exploration of the mathematical foundation and implementation of interval analysis. For simplicity, the numerical interval solution for the direct kinematic problem of this PM is computed by utilizing two Julia packages from the JuliaIntervals ecosystem, IntervalArithmetic and IntervalRootFinding [21].

Next, the velocity analysis was conducted by taking the first derivative of the position equation concerning time. Thus, the Jacobian of direct kinematics and the Jacobian of the inverse kinematics can be obtained concerning this velocity analysis. Both Jacobians hold the key to the singularities of the manipulator, i.e.: the inverse kinematic singularity, the direct kinematic singularity, and the combined singularity.

Consequently, the condition offered by the singularities can be used to construct a workspace for this manipulator. Here, the inverse kinematic singularity gives a boundary of this workspace, which can be called the theoretical workspace. Thus, the presence of a singularity within this workspace can be checked by the condition suggested by the direct kinematic singularity. If this type of singularity exists, then the non-singular or singularity-free workspace can be determined.

The simplest way to determine the singularity-free workspace is through the use of a grid-mesh approach in the cartesian spaces inside the theoretical workspace. This cartesian space is equally divided along each respective axis. Thus, each point can be evaluated to obtain the value of the determinant of the direct kinematic Jacobian. It will give two distinct spaces based on the sign of this evaluated determinant. Here, the boundary of the two spaces is the location of the direct singularity inside the theoretical workspace. One of these two distinct spaces can be identified as the singularity-free workspace. Finally, the evaluation of such workspaces can be performed numerically by using NumPy[22] and then visualized with matplotlib[23].

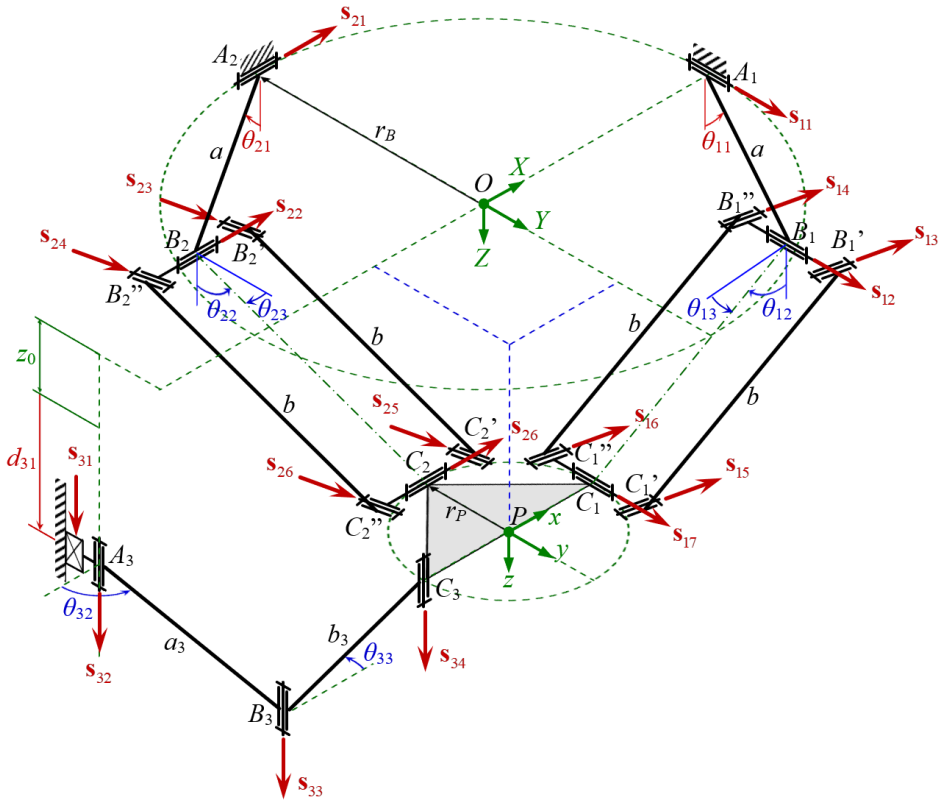

Fig. 1. The 2(RRPaRR)-PRRR parallel kinematic chains or an asymmetric parallel manipulator including its unit direction vector for constructing motion screws (twists) at each joint.

3 Results and Discussion

3.1 Mobility using Grübler-Kutzbach Equation

The mobility of this parallel manipulator can be determined from its kinematic chains that are already shown in Fig. 1. The easiest way to calculate its mobility is the implementation of the Grübler-Kutzbach (GK) equation that highly depends on the number of links and the number of joints. This manipulator is constructed by one fixed ternary link at the base, one moving ternary link as the platform, and three limbs. The first two limbs possess 5 links and 7 joints, while the third one has 3 links and four joints. Hence, the manipulator has 15 links (ℓ) and 18 joints (j) in total. All joints are the lower pairs where each joint restricts 5 degrees of freedom which means allowing one degree of freedom in motion for each (f_i). Thus, its mobility can be computed with Eq. 1.

$$M = 6(\ell - j - 1) + \sum_{i=1}^{18} f_i = -6 \tag{1}$$

This manipulator has a negative value of mobility. In opposite to its actual, the manipulator can undergo translational motion in space, i.e. it has 3 degree of freedom. Hence, the manipulator can be categorized as an over-constrained mechanism. To obtain the actual mobility, one can implement the screw theory that will be described in the next section.

3.2 Mobility using Screw Theory

The application of screw theory is initiated by forming the unit twists on each joint. The unit twists on all revolute joints can be expressed mathematically as Eq. 2

$$\hat{\$}_{ij} = \left(\mathbf{s}_{ij};\quad \mathbf{r}_{ij} \times \mathbf{s}_{ij}\right) \tag{2}$$

where s_{ij} and r_{ij} are the unit direction vector along the revolute axis and the position vector of the joint with respect to point O, respectively. Then, the subscript index for the revolute joints on the first and the second limb is i = 1, 2; and j = 1 to 7, while the third limb is i = 3; and j = 2 to 4. Then, theprismatic joint that exhibits translation has the unit twist $\hat{\$}_{31}$ composed by the dual vector which only consists of the unit direction vector along the prismatic that is stated as Eq. 3.

$$\hat{\$}_{31} = \left(\mathbf{0};\quad \mathbf{s}_{31}\right) \tag{3}$$

Furthermore, the unit vector on each joint described in Eq. 2 and Eq. 3 is stated as $\mathbf{s}_{11} = (0 \;\; 1 \;\; 0)$, $\mathbf{s}_{12} = \mathbf{s}_{17} = \mathbf{s}_{11}$, $\mathbf{s}_{13} = (c\theta_{12} \;\; -s\theta_{12} \;\; 0)$, $\mathbf{s}_{14} = \mathbf{s}_{15} = \mathbf{s}_{16} = \mathbf{s}_{13}$, $\mathbf{s}_{21} = (1 \;\; 0 \;\; 0)$, $\mathbf{s}_{22} = \mathbf{s}_{27} = \mathbf{s}_{21}$, $\mathbf{s}_{23} = (c\theta_{22} \;\; s\theta_{22} \;\; 0)$, $\mathbf{s}_{24} = \mathbf{s}_{25} = \mathbf{s}_{26} = \mathbf{s}_{23}$, $\mathbf{s}_{31} = (0 \;\; 0 \;\; 1)$, and $\mathbf{s}_{32} = \mathbf{s}_{33} = \mathbf{s}_{34} = \mathbf{s}_{31}$. Whilst, the position vector of each joint measured from the point O on the fixed reference of the frame was given respectively by $\mathbf{r}_{i1} = \overrightarrow{OA_i}$, $\mathbf{r}_{i2} = \mathbf{r}_{i1} + \overrightarrow{A_iB_i}$, $\mathbf{r}_{i3} = \mathbf{r}_{i2} + \overrightarrow{B_iB_i'}$, $\mathbf{r}_{i4} = \mathbf{r}_{i2} + \overrightarrow{B_iB_i''}$, $\mathbf{r}_{i5} = \mathbf{r}_{i3} + \overrightarrow{B_iC_i'}$, $\mathbf{r}_{i6} = \mathbf{r}_{i4} + \overrightarrow{B_i''C_i''}$, $\mathbf{r}_{i7} = \mathbf{r}_{i2} + \overrightarrow{B_iC_i}$ for i = 1; 2, $\mathbf{r}_{31} = \mathbf{r}_{32} = \overrightarrow{OA_3}$, $\mathbf{r}_{33} = \mathbf{r}_{31} + \overrightarrow{A_3B_3}$, and $\mathbf{r}_{34} = \mathbf{r}_{33} + \overrightarrow{B_3C_3}$.

The other position vectors given by the previous relations are $\overrightarrow{OA_1} = (r_B \;\; 0 \;\; 0)^T$, $\overrightarrow{OA_2} = (0 \;\; -r_B \;\; 0)^T$, $\overrightarrow{OA_3} = (-x_0 \;\; -y_0 \;\; z_0 + d_{31})^T$, $\overrightarrow{A_1B_1} = a(s\theta_{11} \;\; 0 \;\; c\theta_{11})^T$, $\overrightarrow{A_2B_2} = a(0 \;\; -s\theta_{21} \;\; c\theta_{21})^T$, $\overrightarrow{A_3B_3} = a_3(c\theta_{32} \;\; s\theta_{32} \;\; 0)^T$, $\overrightarrow{B_1B_1'} = (0 \;\; d/2 \;\; 0)^T$, $\overrightarrow{C_1C_1'} = \overrightarrow{B_1B_1'}$, $\overrightarrow{B_2B_2'} = (d/2 \;\; 0 \;\; 0)^T$, $\overrightarrow{C_2C_2'} = \overrightarrow{B_2B_2'}$, $\overrightarrow{B_1B_1''} = \overrightarrow{C_1C_1''} = -\overrightarrow{B_1B_1'}$, $\overrightarrow{B_2B_2''} = \overrightarrow{C_2C_2''} = -\overrightarrow{B_2B_2'}$, $\overrightarrow{B_1C_1} = b(s\theta_{12}c\theta_{13} \;\; -s\theta_{13} \;\; c\theta_{12}c\theta_{13})^T$, $\overrightarrow{B_2C_2} = b(s\theta_{23} \;\; s\theta_{22}c\theta_{23} \;\; c\theta_{22}c\theta_{23})^T$, $\overrightarrow{B_1'C_1'} = \overrightarrow{B_1''C_1''} = \overrightarrow{B_1C_1}$, $\overrightarrow{B_2'C_2'} = \overrightarrow{B_2''C_2''} = \overrightarrow{B_2C_2}$, and $\overrightarrow{B_3C_3} = b_3(c\theta_{33} \;\; s\theta_{33} \;\; 0)^T$. Also, $c\theta_{ij}$ and $s\theta_{ij}$ denote the cosine and sine of θ_{ij}, respectively.

Combining these unit twists within each limb produces the Limb Twist System (LTS) as Eq. 4

$$\begin{aligned}
\hat{\$}_1^{LTS} &= \left[\hat{\$}_{11},\ \hat{\$}_{12},\ \hat{\$}_{13},\ \hat{\$}_{14},\ \hat{\$}_{15},\ \hat{\$}_{16},\ \hat{\$}_{17}\right],\\
\hat{\$}_2^{LTS} &= \left[\hat{\$}_{21},\ \hat{\$}_{22},\ \hat{\$}_{23},\ \hat{\$}_{24},\ \hat{\$}_{25},\ \hat{\$}_{26},\ \hat{\$}_{27}\right],\\
\hat{\$}_3^{LTS} &= \left[\hat{\$}_{31},\ \hat{\$}_{32},\ \hat{\$}_{33},\ \hat{\$}_{34}\right],
\end{aligned} \tag{4}$$

Eq. 4 states that the first two limbs formed a twist of the 7-system and the third one was a twist of the 4-system. Referring to the geometry of the parallelogram chain in the first and the second limb can be understood that both limbs have five-unit twists that are unique or be called twists of a 5-system. Henceforth, these LTSs can be expressed in the unique unit twists, as given as Eq. 5

$$\begin{aligned}
\hat{\$}_1^{LTS} &= \left[\hat{\$}_{11},\ \hat{\$}_{12},\ \hat{\$}_{\mathbf{13}}^{u},\ \hat{\$}_{\mathbf{15}}^{u},\ \hat{\$}_{17}\right],\\
\hat{\$}_2^{LTS} &= \left[\hat{\$}_{21},\ \hat{\$}_{22},\ \hat{\$}_{23}^{u},\ \hat{\$}_{25}^{u},\ \hat{\$}_{27}\right],\\
\hat{\$}_3^{LTS} &= \left[\hat{\$}_{31},\ \hat{\$}_{32},\ \hat{\$}_{33},\ \hat{\$}_{34}\right],
\end{aligned} \tag{5}$$

where the superscript u indicates the unique twist is defined by $\hat{\$}_{13}^{u} = \left(\mathbf{s}_{13};\quad \mathbf{r}_{13}^{u} \times \mathbf{s}_{13}\right)$, $\hat{\$}_{15}^{u} = \left(\mathbf{s}_{15};\quad \mathbf{r}_{15}^{u} \times \mathbf{s}_{15}\right)$, $\hat{\$}_{23}^{u} = \left(\mathbf{s}_{23};\quad \mathbf{r}_{23}^{u} \times \mathbf{s}_{23}\right)$, and $\hat{\$}_{25}^{u} = \left(\mathbf{s}_{25};\quad \mathbf{r}_{ij} \times \mathbf{s}_{ij}\right)$, with $\mathbf{r}_{13}^{u} = \mathbf{r}_{12}$, $\mathbf{r}_{15}^{u} = \mathbf{r}_{17}$, $\mathbf{r}_{23}^{u} = \mathbf{r}_{22}$, and $\mathbf{r}_{25}^{u} = \mathbf{r}_{27}$.

Referring to these LTSs, it can be determined the unit wrenches acting on each limb. Indeed, the reciprocal screw product must be applied to the LTS of each limb to obtain the unit wrench system of each respective limb or LWS. Thus, LWS on the first, second, and third limbs forms a wrench of 1-, 1-, and 2-system, respectively. Mathematically, it is given as Eq. 6

$$\begin{aligned}
\hat{\$}_1^{LWS} &= \left[\hat{\$}_{11}^{LWS}\right],\\
\hat{\$}_2^{LWS} &= \left[\hat{\$}_{21}^{LWS}\right],\\
\hat{\$}_3^{LWS} &= \left[\hat{\$}_{31}^{LWS},\ \hat{\$}_{32}^{LWS}\right],
\end{aligned} \tag{6}$$

where $\hat{\$}_{11}^{LWS} = \left(\mathbf{0};\quad \mathbf{m}_{11}\right)$, $\hat{\$}_{21}^{LWS} = \left(\mathbf{0};\quad \mathbf{m}_{21}\right)$, $\hat{\$}_{31}^{LWS} = \left(\mathbf{0};\quad \mathbf{m}_{31}\right)$, and $\hat{\$}_{32}^{LWS} = \left(\mathbf{0};\quad \mathbf{m}_{32}\right)$ with $\mathbf{m}_{11} = (s\theta_{12} \;\; 0 \;\; c\theta_{12})$, $\mathbf{m}_{21} = (0 \;\; -s\theta_{22} \;\; c\theta_{22})$, $\mathbf{m}_{31} = (1 \;\; 0 \;\; 0)$, and $\mathbf{m}_{32} = (0 \;\; 1 \;\; 0)$. The first and the second limbs have a wrench with shared zero pitch along the Z-axis. Whilst, the third limb has two wrenches with zero pitch along the X and Y-axis. It means that all screws in the LWSs have an infinite pitch that correlates to the restraining moments.

Next, the unit wrenches acting on the platform can be established by taking the union of all LWSs. It gave four unit wrenches that formed the screw of the 4-system. Meanwhile, it is only three unique unit wrenches restrained the platform or the screw of the 3-system. This wrench system is called the PWS and is given by Eq. 7.

$$\hat{\$}^{PWS} = \left[\hat{\$}_{11}^{LWS},\ \hat{\$}_{31}^{LWS},\ \hat{\$}_{32}^{LWS}\right] \tag{7}$$

Finally, applying reciprocal screw product to the PWS will produce the unit twist system in the platform. It is expressed mathematically asEq. 8

$$\hat{\$}^{PTS} = \left[\hat{\$}_1^{PTS},\ \hat{\$}_2^{PTS},\ \hat{\$}_3^{PTS}\right] \tag{8}$$

where $\hat{\$}_i^{PTS} = (\mathbf{0};\ \ \mathbf{s}_i)$ for i = 1; 2; 3, $\mathbf{s}_1 = (1\ \ 0\ \ 0)$, $\mathbf{s}_2 = (0\ \ 1\ \ 0)$, and $\mathbf{s}_3 = (0\ \ 0\ \ 1)$. Hence, referring to this PTS can be known that the platform has twists of the 3-system, where each twist possesses infinite pitch. It means that the platform can undergo translational motion in the *X*-, *Y*-, and *Z*-direction. In other words, the manipulator has a pure translational motion on its platform.

3.3 The Inverse Kinematic Problems

Position of the point *P* on the platform w.r.t. the point *O* as the origin of the fixed reference of frame O-XYZ can be written for each limb as Eq. 9

$$\overrightarrow{OP} = \overrightarrow{OA_i} + \overrightarrow{A_iB_i} + \overrightarrow{B_iC_i} + \overrightarrow{C_iP} \tag{9}$$

for i = 1; 2; 3, where $\overrightarrow{OP} = (x\ \ y\ \ z)^T$, $\overrightarrow{PC_1} = (r_P\ \ 0\ \ 0)^T$, $\overrightarrow{PC_2} = (0\ \ -r_P\ \ 0)^T$, $\overrightarrow{PC_3} = -\overrightarrow{PC_1}$, and $\overrightarrow{C_iP} = -\overrightarrow{PC_i}$. Thus, eliminating the passive joints can be performed by rearranging them into form as Eq. 10.

$$\overrightarrow{OP} + \overrightarrow{PC_i} - \overrightarrow{OA_i} - \overrightarrow{A_iB_i} = \overrightarrow{B_iC_i} \tag{10}$$

The inverse kinematic problem is aimed at seeking the solution of actuated or active joint space for the given values of end-effector space. Referring to this manipulator, the end-effector space is the position of point *P* on the platform, i.e. *x*; *y*; and *z*, and the actuated joint space isθ_{11}, θ_{21}, and d_{31}.

Then, the elimination of the passive joint θ_{12} and θ_{13} for the first limb and θ_{22} and θ_{23} for the second limb can be conducted by applying the dot product for each respective side that yields Eq. 11

$$\begin{aligned} \left(x_1 - a\cdot \mathrm{s}\theta_{11}\right)^2 + y^2 + \left(z - a\cdot \mathrm{c}\theta_{11}\right)^2 &= b^2 \\ x^2 + \left(y_2 + a\cdot \mathrm{s}\theta_{21}\right)^2 + \left(z - a\cdot \mathrm{c}\theta_{21}\right)^2 &= b^2 \end{aligned} \tag{11}$$

where $x_1 = x + r_P - r_B$ and $y_2 = y - r_P + r_B$. Meanwhile, if we are applying the same step as Eq. 11 for the third limb through the application of scalar product for each side will generate the equation in the passive joint of θ_{32}, as given Eq. 12.

$$\begin{aligned} \left(x - r_P - a_3\cdot \mathrm{c}\theta_{32}\right)^2 + \left(y - a_3\cdot \mathrm{s}\theta_{32}\right)^2 \\ + \left(z - z_0 - d_{31}\right)^2 = b_3^2 \end{aligned} \tag{12}$$

Relying on the nature of the third limb, one can know that the limb moves the platform along the *Z*-axis when it is actuated. Consequently, it gives the relation from the *Z*-component (Eq. 13).

$$z - z_0 - d_{31} = 0 \tag{13}$$

Using the solution Eq. 13 can be obtained the solution of the passive joint θ_{32} later on.

Thus, it can be rewritten Eq. 12 and into the following form after applying the half-tangent relations which yields Eq. 14

$$\begin{aligned} 2az\cdot \mathrm{c}\theta_{11} + 2ax_1\cdot \mathrm{s}\theta_{11} &= K_1, \\ 2az\cdot \mathrm{c}\theta_{21} - 2ay_2\cdot \mathrm{s}\theta_{21} &= K_2, \end{aligned} \tag{14}$$

where $K_1 = x_1^2 + y^2 + z^2 + a^2 - b^2$ and $K_2 = x^2 + y_2^2 + z^2 + a^2 - b^2$. The solution for the actuated joints θ_{11} and θ_{21} is given by Eq. 15 and Eq. 16

$$\theta_{11} = 2\tan^{-1}\left(\frac{2ax_1 + \lambda\sqrt{4a^2\left(x_1^2 + z^2\right) - K_1^2}}{K_1 + 2az}\right) \tag{15}$$

$$\theta_{21} = 2\tan^{-1}\left(\frac{-2ay_2 + \lambda\sqrt{4a^2\left(y_2^2 + z^2\right) - K_2^2}}{K_2 + 2az}\right) \tag{16}$$

whereλ = ± 1, andd_{31} given by Eq. 17.

$$d_{31} = z - z_0 \tag{17}$$

These inverse kinematic solutions provide four assembly modes for the manipulator, that depend on the combination of λ, i.e (+1, +1); (+1, -1); (-1, +1); and (-1, -1).

3.4 The Direct Kinematic Problems

Inversely to the inverse kinematic problem, the direct kinematic problem is implemented to seek the solution for the manipulator in the end-effector space (*x*, *y*, and *z*) for the given actuated joint space (θ_{11}, θ_{21}, and d_{31}). It can be determined by utilizing the previous relations in Eq. 11 and Eq. 13. Rewriting those equations gives Eq. 18

$$\begin{aligned} x^2 - 2\delta_1 x + y^2 + \kappa_1^2 &= 0, \\ x^2 + y^2 + 2\delta_2 y + \kappa_2^2 &= 0, \\ z - z_0 - d_{31} &= 0, \end{aligned} \tag{18}$$

where $\delta_1 = r_B - r_P + a\cdot \mathrm{s}\theta_{11}$, $\delta_2 = r_B - r_P + a\cdot \mathrm{s}\theta_{21}$, $\kappa_1^2 = \delta_1^2 + \left(z - a\cdot \mathrm{c}\theta_{11}\right)^2 - b^2$, and $\kappa_2^2 = \delta_2^2 + \left(z - a\cdot \mathrm{c}\theta_{21}\right)^2 - b^2$.

Thence, the solution for *z* can be realized directly from the third equation of Eq. 18, which yields Eq. 19.

$$z = z_0 + d_{31} \tag{19}$$

Meanwhile, the solution for *x* and *y* can be determined by applying the dyalitic elimination method to the first and the second (Eq. 18). Here, *x* and its power are variables in this dyalitic elimination that are given as Eq. 20

$$\begin{bmatrix} 1 & -2\delta_1 & y_\kappa^2 & 0 \\ 1 & 0 & y_{\delta\kappa}^2 & 0 \\ 0 & 1 & -2\delta_1 & y_\kappa^2 \\ 0 & 1 & 0 & y_{\delta\kappa}^2 \end{bmatrix} \begin{Bmatrix} x^3 \\ x^2 \\ x \\ 1 \end{Bmatrix} = \begin{Bmatrix} 0 \\ 0 \\ 0 \\ 0 \end{Bmatrix} \tag{20}$$

where $y_\kappa^2 = y^2 + \kappa_1^2$ and $y_{\delta\kappa}^2 = y^2 + 2\delta_2 y + \kappa_2^2$.

Then, the non-trivial solution of Eq. 20 can be determined by computing the determinant of the 4 by 4 matrix in Eq. 20. Consequently, it produces a quadratic relation in *y* as given Eq. 21

$$\alpha_2 y^2 - \alpha_1 y + \alpha_0 = 0 \tag{21}$$

where $\alpha_2 = 4\left(\delta_1^2 + \delta_2^2\right)$, $\alpha_1 = 4\delta_2\left(\kappa_1^2 - \kappa_2^2 - 2\delta_1^2\right)$, and $\alpha_0 = \left(\kappa_1^2 - \kappa_2^2\right)^2 + 4\delta_1^2\kappa_2^2$. Hence, the solution for *y* can be established easily by solving the quadratic equation (Eq. 21), which yieldsEq. 22.

$$y = \frac{\alpha_1 \pm \sqrt{\alpha_1^2 - 4\alpha_0\alpha_2}}{2\alpha_2} \tag{22}$$

Later, the solution for x is obtained directly from the first equation (Eq. 18) after substituting the solution for z and y. It gives Eq. 23.

$$x = \delta_1 \mp \sqrt{\delta_1^2 - y^2 - \kappa_1^2} \tag{23}$$

Therefore, this manipulator has two unique roots of the direct kinematic problem in the form of a closed-form solution. This solution is analogous to the 2 DoF planar PM with a 5R kinematic chain in term of the highest power of its polynomial equation [24], [25].

To compute the numerical values for the closed-form solution, one can select the kinematic parameters of this PM, which are given numerically as r_B = 200 mm, a = 200 mm, b = 300 mm, and r_P = 100 mm. Afterwards, the closed-form solution in Eq. 19, Eq. 22, and Eq. 23 can be evaluated numerically for the chosen actuator spaces presented in Tables 1 and 2. The aforementioned values are also applicable to the numerical solution obtained using interval analysis. The implementation of interval analysis necessitates an interval box for exploring the search space within the end-effector space.

A brief illustration of the steps to obtain the interval solution using the JuliaInterval ecosystem. Initially, the interval box is selected within the range of [-400, 400] mm, [-400, 400] mm, and [0, 600] mm for the interval in x-, y-, and z-directions, respectively. Subsequently, it is verified whether the solution lies within the interval box. Then, this interval box is divided in half along the longest interval. These new interval boxes are checked again to determine the solution's existence. If the solution exists, the boxes are bisected again. If not, they are discarded. This process is repeated until the relative error of the solution is less than a specified tolerance, which is set to 10^{-16}. Finally, the interval analysis provides two solutions for the direct kinematic problem in the interval boxes, also known as the interval solution.

The interval solution for the direct kinematic problem is listed in Tables 1 and 2, allowing a side-by-side comparison of both solutions. It is worth noting that the maximum range between the lower and the upper bound of each interval solution is less than or equal to 0.001 mm (1 μm). The assessment of the closed-form solution is encompassed within the interval solution, providing evidence that the interval analysis accurately estimates two-pairs solution for the direct kinematic solution. As indicated by the closed-form and interval solutions, the direct kinematic problem is fairly simple in its solution.

Table 1. The first root of the closed-form and interval solution of the direct kinematic problem, the actuator spaces are measured in rad and mm for angular and translational displacement, respectively

Case No	Actuator spaces			Closed-form solution	Interval solution
	θ_{11}	θ_{21}	d_{31}	(x, y, z) mm	[x] × [y] × [z] mm
1	0	0	100	(243.6491673, -243.6491673,100)	[243.649, 243.65] × [-243.65, -243.649]× [100, 100]
2	π/6	π/3	200	(282.4969203, -287.1868563, 200)	[282.496, 282.497] × [-287.187, -287.186] × [200, 200]
3	π/4	π/6	200	(284.5937894, -291.0406905, 200)	[284.593, 284.594] × [-291.041, -291.04] × [200, 200]
4	π/3	π/3	200	(282.6838395, -282.6838395, 200)	[282.683, 282.684] × [-282.684, -282.683] × [200, 200]

Table 2. The second root of closed-form and interval solution of the direct kinematic problem, the actuator spaces are measured in rad and mm for angular and translational displacement, respectively

Case No	Actuator spaces			Closed-form solution	Interval solution
	θ_{11}	θ_{21}	d_{31}	(x, y, z) mm	[x] × [y] × [z] mm
1	0	0	100	(-143.6491673, 143.6491673, 100)	[-143.65, -143.649] × [143.649, 143.65] × [100, 100]
2	π/6	π/3	200	(-98.6901338, -8.1385656, 200)	[-98.6902, -98.6901] × [-8.13857, -8.13856] × [200, 200]
3	π/4	π/6	200	(-36.5071308, 96.5624078, 200)	[-36.5072, -36.5071] × [96.5624, 96.5625] × [200, 200]
4	π/3	π/3	200	(-9.4787588, 9.4787588, 200)	[-9.47876, -9.47875] × [9.47875, 9.47876] × [200, 200]

3.5 Jacobian

Obtaining the Jacobian of this manipulator can be performed by determining the velocity relation between the end-effector velocities and the actuated joint velocities. The simplest way to determine the Jacobian is to take the derivative of the previous equations in Eq. 11 and Eq. 13 with respect to time. Substituting these velocity equations into a compact matrix expression yield Eq. 24

$$\mathbf{J}_q \dot{\mathbf{q}} = \mathbf{J}_x \dot{\mathbf{x}} \tag{24}$$

where $\dot{\mathbf{q}} = \begin{pmatrix} \dot{\theta}_{11} & \dot{\theta}_{21} & \dot{d}_{31} \end{pmatrix}$ is the actuated joint velocities and $\dot{\mathbf{x}} = \begin{pmatrix} \dot{x} & \dot{y} & \dot{z} \end{pmatrix}$ denotes the end-effector velocities.

Then, the inverse and the direct kinematic Jacobian are given respectively by Eq. 25 and Eq. 26

$$\mathbf{J}_q = \begin{bmatrix} J_{q11} & 0 & 0 \\ 0 & J_{q22} & 0 \\ 0 & 0 & 1 \end{bmatrix} \tag{25}$$

$$\mathbf{J}_x = \begin{bmatrix} J_{x11} & y & J_{x13} \\ x & J_{x22} & J_{x23} \\ 0 & 0 & 1 \end{bmatrix} \tag{26}$$

where $J_{q11} = a\left(-x_1 \cdot \mathrm{c}\theta_{11} + z \cdot \mathrm{s}\theta_{11}\right)$, $J_{q22} = a\left(y_2 \cdot \mathrm{c}\theta_{21} + z \cdot \mathrm{s}\theta_{21}\right)$, $J_{x11} = x_1 - a \cdot \mathrm{s}\theta_{11}$, $J_{x13} = z - a \cdot \mathrm{c}\theta_{11}$, $J_{x22} = y_2 + a \cdot \mathrm{s}\theta_{21}$, and $J_{x23} = z - a \cdot \mathrm{c}\theta_{21}$. At last, the Jacobian's manipulator can be determined by computing Eq. 27.

$$\mathbf{J} = \mathbf{J}_q^{-1} \mathbf{J}_x \tag{27}$$

3.6 Singularities

Singularities will exist in this parallel manipulator if either Eq. 25 or Eq. 26 and even both of them degenerates. The degeneration of a matrix shows a condition where its determinant becomes zero or it has a rank of a matrix lower than it should be. The first type of singularity is the inverse kinematic singularity, which is given by the determinant value of the inverse kinematic Jacobian (Eq. 25).

At this singularity, the physical condition of the manipulator for at least one limb – its upper and lower parts – is in extended or folded form. Referring to its physical condition, this singularity occurred at the workspace boundary and manipulator will loose one or more degree of freedom.

Then, the second type of singularity can be found out from Jacobian of the direct kinematics. It shall give the direct kinematic singularity which expressed mathematically by Eq. 29.

The physical intepretation of this manipulator at this singularity is indicated by the lower part of the first two limb being parallel to each other and the platform. Then, this singularity occurs inside the workspace and this manipulator will gain one or more dregrees of freedom.

Moreover, the third type of singularity is called the combined singularity. It occurs when the conditions given by Eq. 28 and Eq. 29 are satisfied simultaneously at the same time. Then, this type of singularity is located at the intersection between the invers and direct kinematic singularity loci.

$$\left|\mathbf{J}_q\right| = J_{q11} \cdot J_{q22} = 0 \tag{28}$$

$$\left|\mathbf{J}_x\right| = J_{x11} \cdot J_{x22} - xy = 0 \tag{29}$$

3.7 Workspaces

The manipulator workspace can first be determined by applying a condition given by Eq. 28 to obtain its boundary. Then, inside this boundary, the manipulator's workspace will later be known as the theoretical workspace. Unfortunately, that workspace suffers from the existence of the direct kinematic singularity as given by Eq. 29. Hence, it makes the workspace smaller than the previous condition that given by Eq. 28 itself. This workspace is known as the non-singular or singularity-free workspace.

This singularity-free workspace can be determined by examining several numerical values of the kinematic parameters, i.e. r_B, r_P, a, and b. One can take the non-dimensional value of those kinematic parameters for simplification while evaluating that workspace. Altering those four parameters into the non-dimensional ones can be done directly by applying the Eq. 30.

$$r_B + a + b + r_P = 4 \tag{30}$$

Finally, the non-dimensional values for determining the manipulator's workspace with 2(RRPaRR)-PRRR kinematic chain are selected for two cases as listed in Table 3.

Table 3. The non-dimensional values for the kinematic parameters of the manipulator with 2(RRPaRR)-PRRR kinematic chain

Case No	r_B	a	b	r_P
1	1.00	1.00	1.80	0.20
2	1.00	1.40	1.40	0.20

The theoretical workspace can be determined by applying a grid-mesh approach for each non-dimensional value of the kinematic parameter. Thus, this workspace can be divided into two distinct workspaces based on the sign of the determinant of (Eq. 26). These workspaces can be visualized most simply by taking the slices of the workspace on each plane, i.e.: *xy*-plane, *yz*-plane, and *xz*-plane – instead of visualizing the entire workspace – as shown in Fig. 2.

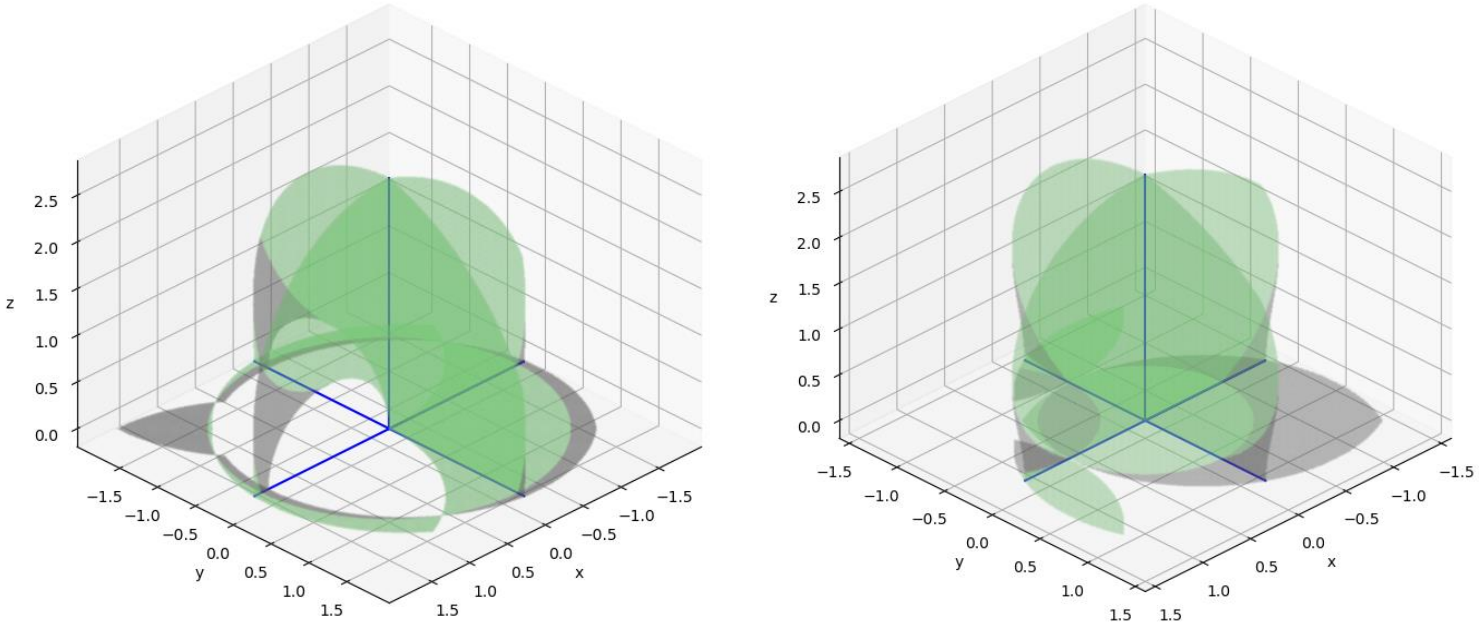

(a) Case 1 (b) Case 2

Fig. 2. The workspace of the manipulator for each kinematic parameter that is given in Table 3 for both cases.

The part of the theoretical workspace in either the transparent light gray or the transparent light green represents a non-continuous workspace. The boundary between these two colors corresponds to the locus of the direct kinematic singularity as expressed by Eq. 29. However, the part with the transparent light green color has more significant part near the center as a continuous workspace. Therefore, this larger part can be used as the singularity-free workspace. In practice, not all singularity-free workspace will be available as useful ones. Moreover, the notion of useful workspace presented here is not the workspace that is evaluated by any performance metrics, such as condition index, transmission index, dexterity index, and so on.

Overall, the analysis demonstrated in this article shows the applicability of the asymmetric PM with 2(RRPaRR)-PRRR kinematic chains. This PM belongs to the overconstrained manipulator that offers high stiffness and payload capacity but presents complexities in force analysis and stiffness modeling [26], [27]. Significantly, this PM has simple inverse and direct kinematic solutions that can be determined from its closed-form solution. Referring to its workspace, the PM provides a singularity-free workspace that has irregular shapes compared to its counterpart, DELTA [28] or Tripteron[14].

4 Conclusion

This research has been carried out to investigate the mobility, kinematics, singularity, and workspace analysis of a proposed asymmetric PM with 2(RRPaRR)-PRRR kinematic chain. The mobility analysis via screw theory shows that this PM has 3 DoF in space for all translational motions, known as a pure translational PM. Then, the inverse kinematic analysis of this PM gives the closed-form solution that provides four assembly modes for its working modes. Also, the direct kinematic analysis yields a

closed form solution in a simple quadratic equation. It means that this PM has two direct kinematic configurations. The same result is obtained through the use of interval analysis.

Furthermore, this PM can experience the three kinds of singularities. First is the inverse kinematic singularity, which occurs at the workspace boundary. Second, the direct kinematic singularity exists inside the workspace, which divides it into several regions bounded by its singularity loci. The third kind of singularity, or the combined singularity, happens at the intersection of the singularity loci between the inverse and the direct kinematic ones. Then, using the workspace visualization, the singularity-free workspace that lies around the z-axis of this PM can be identified. In the near future, the dimensional synthesis of this PM will be performed in order to maximize its useful workspace, which is subject to constraints such as the non-singularity workspace, the conditioning index, and the motion/transmission index.

Acknowledgements

The authors would like to express their sincere gratitude to the MajelisDiktilitbang PP Muhammadiyah who funded this research under a grant from the PenelitianDasarRisetMU, Contract No. 1687.241/PD/I.3/D/2022. We are also grateful to the reviewers who provided blind peer review and corrections to this manuscript.

References

[1] Z. Pandilov and V. Dukovski, "Comparison of the Characteristics Between Serial and Parallel Robots," *Acta Teh. Corviniensis - Bull. Eng.*, vol. VII, no. 1, pp. 143–160, 2014.

[2] S. Lu and Y. Li, "Dimensional Synthesis of a 3-DOF Translational Parallel Manipulator Considering Kinematic Dexterity Property," vol. 183, no. July, 2014.

[3] A. Karimi, M. Tale, and P. Cardou, "Avoiding the singularities of 3-RPR parallel mechanisms via dimensional synthesis and self-reconfigurability," *MAMT*, vol. 99, pp. 189–206, 2016, doi: 10.1016/j.mechmachtheory.2016.01.006.

[4] M. Russo, L. Raimondi, X. Dong, D. Axinte, and J. Kell, "Task-oriented optimal dimensional synthesis of robotic manipulators with limited mobility," *Robot. Comput. Integr. Manuf.*, vol. 69, pp. 1–18, 2021, doi: 10.1016/j.rcim.2020.102096.

[5] Z. Yang and D. Zhang, "Novel Design of a 3-RRUU 6-DOF Parallel Manipulator," in *2018 4th International Conference on Mechanical and Aeronautical Engineering. In IOP Conference Series: Materials Science and Engineering*, 2019, vol. 491, pp. 1–10, doi: 10.1088/1757-899X/491/1/012006.

[6] W. Ye and Q. Li, "Type Synthesis of Lower Mobility Parallel Mechanisms: A Review," *Chinese J. Mech. Eng. (English Ed.*, vol. 32, no. 1, 2019, doi: 10.1186/s10033-019-0350-x.

[7] R. Clavel, "Conception d'un robot parallèle rapide à 4 degrés de liberté," École Polytechnique Fédérale de Lausanne, 1991.

[8] A. H. Dastjerdi, M. M. Sheikhi, and M. T. Masouleh, "A complete analytical solution for the dimensional synthesis of 3-DOF delta parallel robot for a prescribed workspace," *Mech. Mach. Theory*, vol. 153, pp. 1–17, 2020, doi: 10.1016/j.mechmachtheory.2020.103991.

[9] J. Brinker, B. Corves, and Y. Takeda, *Kinematic and dynamic dimensional synthesis of extended delta parallel robots*, vol. 72. Springer International Publishing, 2019.

[10] Y. Li, D. Shang, and Y. Liu, "Kinematic modeling and error analysis of Delta robot considering parallelism error," *Int. J. Adv. Robot. Syst.*, vol. 16, no. 5, pp. 1–9, 2019, doi: 10.1177/1729881419878927.

[11] D. Shang, Y. Li, Y. Liu, and S. Cui, "Research on the motion error analysis and compensation strategy of the Delta robot," *Mathematics*, vol. 7, no. 5, 2019, doi: 10.3390/math7050411.

[12] Y. Li, D. Shang, X. Fan, and Y. Liu, "Motion reliability analysis of the delta parallel robot considering mechanism errors," *Math. Probl. Eng.*, pp. 1–10, 2019, doi: 10.1155/2019/3501921.

[13] M. Santhakumar, P. Sunilkumar, L. A. Rybak, D. Malyshev, S. Khalapyan, and A. V. Nozdracheva, "Conceptual Design and Control of a Sitting-Type Lower-Limb Rehabilitation System Established on a Spatial 3-PRRR Parallel Manipulator," in *Zeghloul, S., Laribi, M., Sandoval Arevalo, J. (eds) Advances in Service and Industrial Robotics. RAAD*, Mechanisms., Springer, 2020, pp. 345–355.

[14] I. John, P. Sunilkumar, S. Mohan, and L. A. Rybak, "Investigation of Interference-Free Workspace of a Cartesian (3-PRRR) Parallel Manipulator," in *IFToMM Symposium on Mechanism Design for Robotics. In Mechanism Design for Robotics: MEDER 2021*, 2021.

[15] I. John, S. Mohan, and L. A. Rybak, "Numerical investigations, development and control of a cartesian (3-PRRR) parallel manipulator," *Proc. Inst. Mech. Eng. Part C J. Mech. Eng. Sci.*, vol. 236, no. 15, pp. 8635–8649, 2022.

[16] H. Shen, C. Wu, G. Wu, D. Chablat, and T. li Yang, "Topological design of an asymmetric 3-translational parallel mechanism with zero coupling degree and motion decoupling," in *Proceedings of the ASME 2018 International Design Engineering Technical Conferences and Computers and Information in Engineering Conference*, 2018, pp. 1–8, doi: 10.1115/DETC201885709.

[17] Y. Yang, Y. Tang, H. Chen, Y. Peng, and H. Pu, "Mechanism design and parameter optimization of a new asymmetric translational parallel manipulator," *Mech. Sci.*, vol. 10, pp. 255–272, 2019.

[18] R. E. Moore, R. B. Kearfott, and M. J. Cloud, *Introduction to Interval Analysis*. Society for Industrial and Applied Mathematics, 2009.

[19] J. Merlet, "Interval Analysis and Reliability in Robotics," *Int. J. Reliab. Saf.*, vol. 3, no. 1–3, pp. 104–130, 2009.

[20] J.-P. Merlet, "Interval Analysis for Certified Numerical Solution of Problems in Robotics," *Int. J. Appl. Math. Comput. Sci.*, vol. 19, no. 3, pp. 399–412, 2009, doi: 10.2478/v10006-009-0033-3.

[21] L. Benet and D. P. Sanders, "JuliaIntervals - Guaranteed computations." 2022.

[22] C. R. Harris *et al.*, "Array programming with NumPy," *Nature*, vol. 585, no. 7825, pp. 357–362, 2020, doi: 10.1038/s41586-020-2649-2.

[23] J. D. Hunter, "Matplotlib: A 2D graphics environment," *Comput. Sci. Eng.*, vol. 9, no. 3, pp. 90–95, 2007, doi: 10.1109/MCSE.2007.55.

[24] F. Andres *et al.*, "Kinematic performance of planar 5R symmetrical parallel mechanism subjected to clearances and uncertainties," *J. Brazilian Soc. Mech. Sci. Eng.*, vol. 40, no. 4, pp. 1–15, 2018, doi: 10.1007/s40430-018-1118-4.

[25] Adriyan and A. Yanto, "The Accuracy Bound for Positioning the 5R Planar Parallel Manipulator Subjected to Uncertainties in Dimensions and Actuations," *J. Tek. Mesin*, vol. 12, no. 1, pp. 1–10, 2022.

[26] Y. Xu, W. Liu, J. Yao, and Y. Zhao, "A method for force analysis of the overconstrained lower mobility parallel mechanism," *Mech. Mach. Theory*, vol. 88, pp. 31–48, 2015, doi: 10.1016/j.mechmachtheory.2015.01.004.

[27] W. Cao, H. Ding, and W. Zhu, "Stiffness modeling of overconstrained parallel mechanisms under considering gravity and external payloads," *Mech. Mach. Theory*, vol.

135, pp. 1–16, 2019, doi: 10.1016/j.mechmachtheory.2018.12.031.
[28] J. Brinker, B. Corves, and Y. Takeda, "Kinematic performance evaluation of high-speed Delta parallel robots based on motion/force transmission indices," *Mech. Mach. Theory*, vol. 125, pp. 1–15, 2018, doi: 10.1016/j.mechmachtheory.2017.11.029.